KRONOS FUSION ENERGY

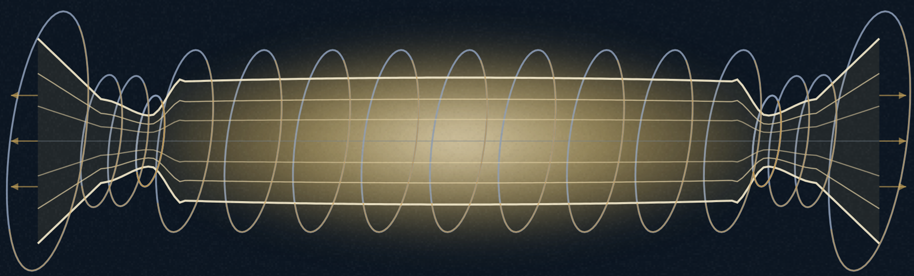

PAPER 2.62 · THE KRONOS 2026 SERIES

The Neutron-Lean Siting Case for a D–^{3}He Tandem-Mirror Burner: Parasitic D–D/D–T Neutron Budgets, Shielded Housing Dose, and Tritium-Suppressed Operation for Defense and Urban Deployment

Where a fusion machine may be built is decided largely by its neutrons, and the Kronos burner is neutron-lean by design so that it can be sited where a conventional D–T source...

Read it live — 3-D model · physics validator · film series

BY P I FORD AND G L KULCINSKI

2026 · EDITORIAL EDITION

THE OFFICIAL RECORD

What this document is, and how to read its numbers

This is a combined editorial. It gathers, in one volume, the two design studies Kronos Fusion Energy released in 2026 — a compact spherical-tokamak tritium/helium-3 breeder and a deuterium–helium-3 tandem-mirror generator — together with the intellectual-property estate, the people, and, in the internal edition, the full commercial case. The scientific text is the same text that appears in the arXiv preprints and the journal submissions; the editorial adds the apparatus a reader needs to hold the whole program at once, and nothing in the physics is altered to fit it.

THE HONESTY STANCE IS THE ASSET

Every headline quantity carries an **evidence class** — DERIVED RECOMPUTED MEASURED REQUIREMENT — and, where a number is a modelled extrapolation rather than a demonstrated value, it is labelled as such and its downside is shown next to it. Several quantities in the underlying corpus moved after first publication; where a value has been withdrawn or restated, the record says so plainly. This is deliberate: a diligence team will find the load-bearing assumptions, so the document surfaces them first.

TWO EDITIONS

This volume is issued in two editions. The **public edition** (light) carries the physics and the design only — no dollar, price, or per-kilogram figure appears anywhere in it. The **internal edition** (dark) adds the economics, the funding architecture, and the defense-commercial analysis, and is marked *Confidential* accordingly; it is not for public distribution. Where the commercial case rests on a modelled assumption rather than a demonstrated one, it is labelled as such and its downside is shown alongside it, on the same terms as the physics.

TITLE	The Kronos Fleet — Hyperion · Aegis · MetroVolt: A Combined Design & Commercialization Study
AUTHOR	Priyanca Ford, Founder & CEO, on behalf of Kronos Fusion Energy
EDITION	2026 Combined Editorial · first issue
COMPANION WORKS	The five-paper arXiv drop — (1) Breeder, (2) Burner, (3) REBCO magnet & tape, (4) Direct Energy Conversion, (5) AI/ML/Quantum control — with matching numbered Zenodo deposits, plus the IOP journal and IAEA-FEC submissions. Patents were filed before the drop.
NAMING	Hyperion = the breeder; Aegis (defense) and MetroVolt (data-center) = one generator in two housings. Internal mode letters (D1, L) do not appear on public surfaces.
STATUS	Conceptual design & simulation study. Nothing herein is a construction commitment.

HOW TO READ THIS VOLUME

The fleet at a glance, and the way its numbers are marked

This volume opens with *Orientation*, presents the five research papers as a bound sequence, and closes with the *Apparatus*. *Foundations* sets out the three general results both machines rest on. *Paper One* is the Hyperion breeder; *Paper Two* the Aegis / MetroVolt generator; *Papers Three, Four and Five* are the enabling science — high-field REBCO magnets and tape, direct energy conversion, and the AI / ML / quantum control stack. A *Digital Twin & 3-D Model* part follows, then the *Environmental* profile. The *Economics* and levelized cost and the *Business Case* and diligence record appear in the internal edition only; the *Simulations* proof record and the Apparatus — patent portfolio, team, limitations, and sources — close both editions.

THE FLEET AT A GLANCE

	HYPERION	AEGIS	METROVOLT
Role	Strategic-isotope foundry	Defense installation power	Campus power
Machine	**Spherical tokamak**	**Tandem mirror**	**Tandem mirror**
Fuel	Deuterium–tritium	Deuterium–helium-3	Deuterium–helium-3
Delivers	Tritium · ^{3}He · 14 MeV n	Resilient installation power	Firm campus power
Physics bar	**Fusion gain only**	Closure (gates named)	Closure + lunar ^{3}He
In the fleet	Breeds the fuel	Proves the generator	Commercial destination

HOW THE NUMBERS ARE MARKED

Every headline quantity carries an evidence class — DERIVED from first principles, RECOMPUTED from raw data, MEASURED in hardware, or a REQUIREMENT yet to be met. Financial figures carry a case label and are confined to the internal (confidential) edition. Values that moved after first publication are shown as withdrawn or restated rather than quietly changed. A capability you can evaluate is one whose limits are on the page.

ABSTRACT

The Neutron-Lean Siting Case for a D–³He Tandem-Mirror Burner: Parasitic D–D/D–T Neutron Budgets, Shielded Housing Dose, and Tritium-Suppressed Operation for Defense and Urban Deployment

Where a fusion machine may be built is decided largely by its neutrons, and the Kronos burner is neutron-lean by design so that it can be sited where a conventional D–T source cannot. *Problem:* the D–^{3}He cycle is only *predominantly* aneutronic — a residual neutron budget survives from unavoidable D–D reactions and from the D–T self-burn of the tritons those reactions breed — and a defensible siting case must resolve that budget, fix it to a self-consistent operating point, and translate it into a dose at the fence and a mobile radioactive inventory. *Method:* we derive the parasitic neutron budget from a steady-state triton-kinetics balance, reducing it to a single master law $P_n = P_{\rm DD}\,[1 + f_{\rm burn} E_n^{\rm DT}/E_n^{\rm DD}]$ in which the in-situ triton burnup fraction $f_{\rm burn}$ is an explicit, physical control variable; we close the operating point with a bremsstrahlung-plus-three-model-synchrotron radiation-transport solution; and we develop a point-kernel dose model and a residence-time tritium-inventory model, all anchored to frozen results reproduced on the NVIDIA GPU HPC campaign (KRONOS Toolkit mirror solver; OpenMC/ENDF-B-VIII.0). *Result:* at the canonical point ($Q_E = 1.318$, $P_{\rm fus} = 4298.5$ MW) only $f_n = 5.44\,\%$ of the power is carried by neutrons ($P_n = 233.95$ MW), a wall-averaged loading of 0.098 MW m^{-2}, one to two orders below a D–T first wall. The 14.03 MeV D–T line carries $60\,\%$ of the neutron power but only $21\,\%$ of the count and therefore sets the shield basis; both shares fall out of a single burnup fraction $f_{\rm burn} \approx 0.26$. A burn-lean mode that pumps bred tritium strips $60\,\%$ of the neutron power ($234 \to 93.5$ MW, to the D–D floor) for a $4.1\,\%$ fusion-power penalty — a $14.6{:}1$ lever. A point-kernel calculation gives a public dose of $\sim 0.11\,\mu$Sv h^{-1} at 50 m behind 2.80 m of concrete (versus 3.06 m for a D–T source; the saving is only logarithmic in source strength), and the licensing-relevant *mobile* tritium inventory is ~ 3.6 g against ~ 1 kg for a D–T plant, a source term $\sim 275\times$ smaller. *Significance:* the same neutron-lean source underwrites both a fixed-defense and an urban, demand-adjacent housing.

Open-access deposit (code & data, CC BY 4.0): DOI 10.5281/zenodo.22645917 · Zenodo community *kronos_fusion_energy*. Explore it live: interactive 3-D model · physics validator.

Keywords: neutron budget · D--^{3}He · aneutronic fusion · shielding · tritium source term · tandem-mirror burner · urban and defense siting

CONTENTS

Table of Contents

NOMENCLATURE

Symbols, units, and the names of things

Q	plasma (fusion) gain, P_{fus}/P_{aux}
Q_E	engineering gain, net electric out / recirculating in
H_{98}	confinement enhancement over the IPB98(y,2) scaling
Z_{eff}	effective ion charge
c_{ee}	electron–electron bremsstrahlung leading coefficient, 2.120022 (exact)
τ_E	energy confinement time
I_p	plasma current
R_0, a	major radius, minor radius
κ, δ	elongation, triangularity
β_N	normalized plasma beta (Troyon-normalized)
TBR	tritium breeding ratio
DEC	direct energy conversion
CF	plant capacity factor (availability)
FOAK / NOAK / BOAK	first / n^{th} / best of a kind
Hyperion	the ST breeder (internal: Mode D2)
Aegis	the generator, defense/installation housing (internal: Mode M)
MetroVolt	the generator, data-center housing (Mode M)

§ 1

Introduction

SITING IS A NEUTRONICS PROBLEM

The location a fusion plant can occupy is set, more than by any other single property, by the neutrons it emits. A conventional deuterium–tritium (D–T) source converts about four-fifths of its fusion power into 14.1 MeV neutrons; it drives its first wall at several megawatts per square metre, activates its structure to contact-handled or remote-handled waste classes, and circulates a kilogram-scale tritium inventory. Each of those properties pushes a D–T plant toward a remote, generously buffered, heavily licensed site. A machine intended to sit on a defense forward base or inside an urban, demand-adjacent campus must break out of that regime at the level of the fuel cycle, not merely by adding shielding.

The Kronos burner is a D–^{3}He tandem mirror designed for exactly that purpose. It is one of two housings — a fixed-defense unit (Aegis) and a data-centre unit (MetroVolt) — built on a common neutron-lean source [2,3]. Its engineering gain and recirculation close at $Q_E = 1.318$ with charged-particle power recovered directly at a direct-energy-converter efficiency $\eta_{\rm DEC} = 0.49$ [9], and its confinement rests on an electrostatically plugged central cell whose ambipolar potential is sustained by hot-electron and sloshing-ion physics behind 26.49 T end-plug coils [7,8]. What makes it *sitable*, however, is that the D–^{3}He reaction

$$\mathrm{D} + {}^3\mathrm{He} \;\longrightarrow\; \mathrm{p}\,(14.68\ \mathrm{MeV}) + {}^4\mathrm{He}\,(3.67\ \mathrm{MeV}), \qquad Q = 18.35\ \mathrm{MeV},$$

releases its entire yield in charged particles. If the plasma burned only reaction (1) it would emit no neutrons at all.

WHY D–^{3}HE IS NOT ANEUTRONIC IN PRACTICE

A real D–^{3}He plasma is not a pure D–^{3}He plasma. The deuterium fuel reacts with itself, and the products of those side reactions react further, so a residual — but structured and, as we show, controllable — neutron budget survives. The advanced-fuel scorecard that motivates the fuel choice makes this explicit: D–^{3}He is the practical near-aneutronic option, far leaner than D–T but not truly neutron-free, and its neutron penalty is dominated by the parasitic deuterium channels rather than by the primary reaction [4,13,14]. The relevant side reactions are the two branches of D–D,

$$\begin{aligned} \mathrm{D} + \mathrm{D} &\longrightarrow \mathrm{n}\,(2.45\ \mathrm{MeV}) + {}^3\mathrm{He}\,(0.82\ \mathrm{MeV}), \qquad Q = 3.27\ \mathrm{MeV},\\ \mathrm{D} + \mathrm{D} &\longrightarrow \mathrm{p}\,(3.02\ \mathrm{MeV}) + \mathrm{T}\,(1.01\ \mathrm{MeV}), \qquad Q = 4.03\ \mathrm{MeV}, \end{aligned}$$

which occur with nearly equal branching, and the D–T reaction that the triton branch (2) feeds,

$$\mathrm{D} + \mathrm{T} \;\longrightarrow\; \mathrm{n}\,(14.03\ \mathrm{MeV}) + {}^4\mathrm{He}\,(3.52\ \mathrm{MeV}), \qquad Q = 17.59\ \mathrm{MeV}.$$

The neutron output therefore has two lines: a soft 2.45 MeV line straight from the D–D neutron branch (2), and a hard 14.03 MeV line from the self-burn of bred tritium (3). This structure is decisive. The two lines differ in energy by a factor of 5.7, so they weigh very differently in shielding and damage even when their reaction rates are comparable; and the hard line is fed by a species — tritium — that can be pumped, which turns the neutron output into something a plant operator can actively lower. Physics of magnetic mirrors and of D–^{3}He reactors has long recognised the aneutronic promise and the D–D floor that limits it [16,17,15]; what has been missing for a specific, buildable machine is a resolved, operating-point-consistent budget and its translation into a siting case.

CONTRIBUTION

This paper supplies that translation for the Kronos burner. We (i) derive the parasitic neutron budget from a formal steady-state triton-kinetics balance and reduce it to a single master law in which the in-situ triton burnup fraction $f_{\rm burn}$ is an explicit control variable (§2); (ii) show that the 60/40 power split and the 21/79 count split between the hard and soft lines both follow from one value of $f_{\rm burn}$, and that the 14 MeV line sets the shield basis despite being the minority by count (§2); (iii) close the operating point with a self-consistent radiation-transport solution that pins the electron temperature (§3); (iv) develop the point-kernel dose formalism and a residence-time mobile-tritium model, and derive the exponential shield law that makes the shield saving only logarithmic in source strength (§4); (v) describe the NVIDIA GPU HPC campaign and reference codes that produced and verified the numbers (§5); and (vi) present the resolved budget, the burn-lean lever, the shield and source-term curves, and the two-housing conclusion (§6–§10). Every quantitative claim traces to a frozen serial in the Kronos Physics De-Risking Register [1]; identifiers (BV-07, KX-L1-A3-BU, AG-CX-16, MV-CX-28, MV-CX-29) are given inline so each number is auditable.

§ 2

Governing equations: the parasitic neutron budget

REACTION NETWORK AND RATE DENSITIES

Let n_D, $n_{\rm He}$, n_T be the deuteron, helium-3 and triton number densities and $\langle\sigma v\rangle_X$ the Maxwellian-averaged reactivity of channel X at the local ion temperature [12]. The volumetric reaction-rate densities are

$$R_{D{\rm He}} = n_D n_{\rm He}\langle\sigma v\rangle_{D{\rm He}}, \qquad R_{DD} = \tfrac{1}{2}\, n_D^2\langle\sigma v\rangle_{DD}, \qquad R_{DT} = n_D n_T\langle\sigma v\rangle_{DT},$$

where the factor $\frac{1}{2}$ in R_{DD} removes the double count of identical reactants and $\langle\sigma v\rangle_{DD}$ is the *total* D–D reactivity summed over both branches. The neutron and triton branches take fractions b_n and $b_T = 1 - b_n$ of R_{DD}; at the ion temperatures of interest the branching is close to even, $b_n \simeq b_T \simeq \frac{1}{2}$, and we carry b_n, b_T symbolically and set them to $\frac{1}{2}$ only in the numerical closure. The primary reaction (1) and the minor ^{3}He–^{3}He channel are aneutronic and do not enter the neutron budget except through the deuterium they consume.

STEADY-STATE TRITON KINETICS AND THE BURNUP FRACTION

Tritons are *born* by the D–D triton branch (2) and *destroyed* either by burning in reaction (3) or by being pumped and transported out of the burning volume. Their zero-dimensional balance is

$$\frac{{\rm d}n_T}{{\rm d}t} = b_T R_{DD} \;-\; \frac{n_T}{\tau_p^*} \;-\; n_D n_T\langle\sigma v\rangle_{DT},$$

where τ_p^* is the effective non-burn triton removal time (active divertor/pump throughput plus confinement loss). Defining the triton burn time

$$\tau_{\rm burn} \equiv \big(n_D\langle\sigma v\rangle_{DT}\big)^{-1},$$

the steady state ($\dot n_T = 0$) of (5) is $n_T = b_T R_{DD}/(\tau_p^{*-1} + \tau_{\rm burn}^{-1})$, and the fraction of bred tritons that burn *in situ* is

$$\boxed{f_{\rm burn} \equiv \frac{R_{DT}}{b_T R_{DD}} = \frac{\tau_{\rm burn}^{-1}}{\tau_p^{*-1} + \tau_{\rm burn}^{-1}} = \frac{\tau_p^*}{\tau_p^* + \tau_{\rm burn}} = \frac{1}{1 + \tau_{\rm burn}/\tau_p^*}}\,.$$

Equation (7) is the hinge of the whole analysis. It is monotone in the pump time: slow pumping ($\tau_p^* \gg \tau_{\rm burn}$) gives $f_{\rm burn} \to 1$ and the tritium mostly burns; aggressive pumping ($\tau_p^* \ll \tau_{\rm burn}$) gives $f_{\rm burn} \to 0$ and the hard neutron line is starved of fuel. The design point sits at an intermediate value fixed below.

NEUTRON SOURCE STRENGTH, COUNT AND POWER

The volumetric neutron source is the sum of the D–D neutron branch and the D–T self-burn,

$$s_n = b_n R_{DD} + R_{DT} = R_{DD}\big(b_n + f_{\rm burn}\, b_T\big),$$

using (7). Integrating over the burning volume V with volume-averaged rate $\bar R_{DD}$ gives the total neutron rate $S_n = \bar R_{DD} V(b_n + f_{\rm burn} b_T) = 3.0\times10^{20}$ s^{-1} (BV-07). The two lines carry neutron energies $E_n^{\rm DD} = 2.45$ MeV and $E_n^{\rm DT} = 14.03$ MeV, so the *count* shares of the hard and soft lines are

$$\chi_{\rm DT} = \frac{f_{\rm burn} b_T}{b_n + f_{\rm burn} b_T}, \qquad \chi_{\rm DD} = \frac{b_n}{b_n + f_{\rm burn} b_T},$$

while the total neutron *power* is

$$P_n = V\big(b_n R_{DD} E_n^{\rm DD} + f_{\rm burn} b_T R_{DD} E_n^{\rm DT}\big).$$

Writing the D–D neutron floor as $P_{\rm DD} \equiv b_n \bar R_{DD} V\, E_n^{\rm DD}$ and setting $b_n = b_T = \frac{1}{2}$, equation (10) collapses to a one-parameter master law,

$$\boxed{P_n(f_{\rm burn}) = P_{\rm DD}\Big[1 + f_{\rm burn}\,\frac{E_n^{\rm DT}}{E_n^{\rm DD}}\Big] = P_{\rm DD}\big[1 + 5.73\, f_{\rm burn}\big]}\,.$$

The whole neutron budget is thus governed by two numbers: the D–D floor $P_{\rm DD}$, set by the deuterium content and reactivity, and the burnup fraction $f_{\rm burn}$, set by the pump balance (7).

FIXING THE DESIGN POINT

The frozen result $P_n = 233.95$ MW with a D–D floor $P_{\rm DD} = 93.5$ MW (BV-07) inverts (11) to

$$f_{\rm burn} = \frac{E_n^{\rm DD}}{E_n^{\rm DT}}\left(\frac{P_n}{P_{\rm DD}} - 1\right) = \frac{1}{5.73}\left(\frac{233.95}{93.5} - 1\right) = 0.263,$$

in agreement, to within the D–D branching ratio, with the register's independent estimate that $\sim 31\,\%$ of self-generated tritium burns in situ (MV-CX-29). With this single value the count and power splits of (9)–(11) evaluate to

$$\chi_{\rm DT} = \frac{0.263}{1 + 0.263} \times \tfrac{1}{1} = 0.208, \qquad \frac{P_n^{\rm DT}}{P_n} = \frac{f_{\rm burn} E_n^{\rm DT}}{E_n^{\rm DD} + f_{\rm burn} E_n^{\rm DT}} = 0.601,$$

i.e. the 14 MeV line is $21\,\%$ of the count but $60\,\%$ of the power, and the 2.45 MeV line is $79\,\%$ of the count and $40\,\%$ of the power (Table 1, Figure 1). Because shielding attenuation and displacement damage both scale steeply with neutron energy, the hard line sets the shield and activation basis *even though most neutrons are soft* — a distinction a single scalar "neutron flux" would erase. Spreading P_n over the first-wall area $A_w = 2378\,\mathrm{m}^2$ gives the wall-averaged neutron loading

$$\Gamma_n = \frac{P_n}{A_w} = \frac{233.95\ \mathrm{MW}}{2378\ \mathrm{m}^2} = 0.098\ \mathrm{MW\,m^{-2}},$$

below the $0.1\,\mathrm{MW\,m^{-2}}$ threshold and one to two orders of magnitude under a D–T first wall — the single most consequential number in the siting case.

LINE	SOURCE	NEUTRON ENERGY	POWER SHARE	COUNT SHARE
hard (D–T self-burn)	eq. (3)	14.03 MeV	140.4 MW ($60\,\%$)	$21\,\%$
soft (D–D)	eq. (2)	2.45 MeV	93.5 MW ($40\,\%$)	$79\,\%$
total	—	—	233.95 MW	$100\,\%$

Burner neutron budget by energy line (BV-07). Total $P_n = 233.95$ MW, $f_n = 5.44\,\%$, total rate $S_n = 3.0 \times 10^{20}\ \mathrm{s^{-1}}$; wall-averaged loading $\Gamma_n = 0.098\ \mathrm{MW\,m^{-2}}$ over $A_w = 2378\,\mathrm{m}^2$. Both shares follow from the single burnup fraction $f_{\rm burn} = 0.263$ of equation (12).

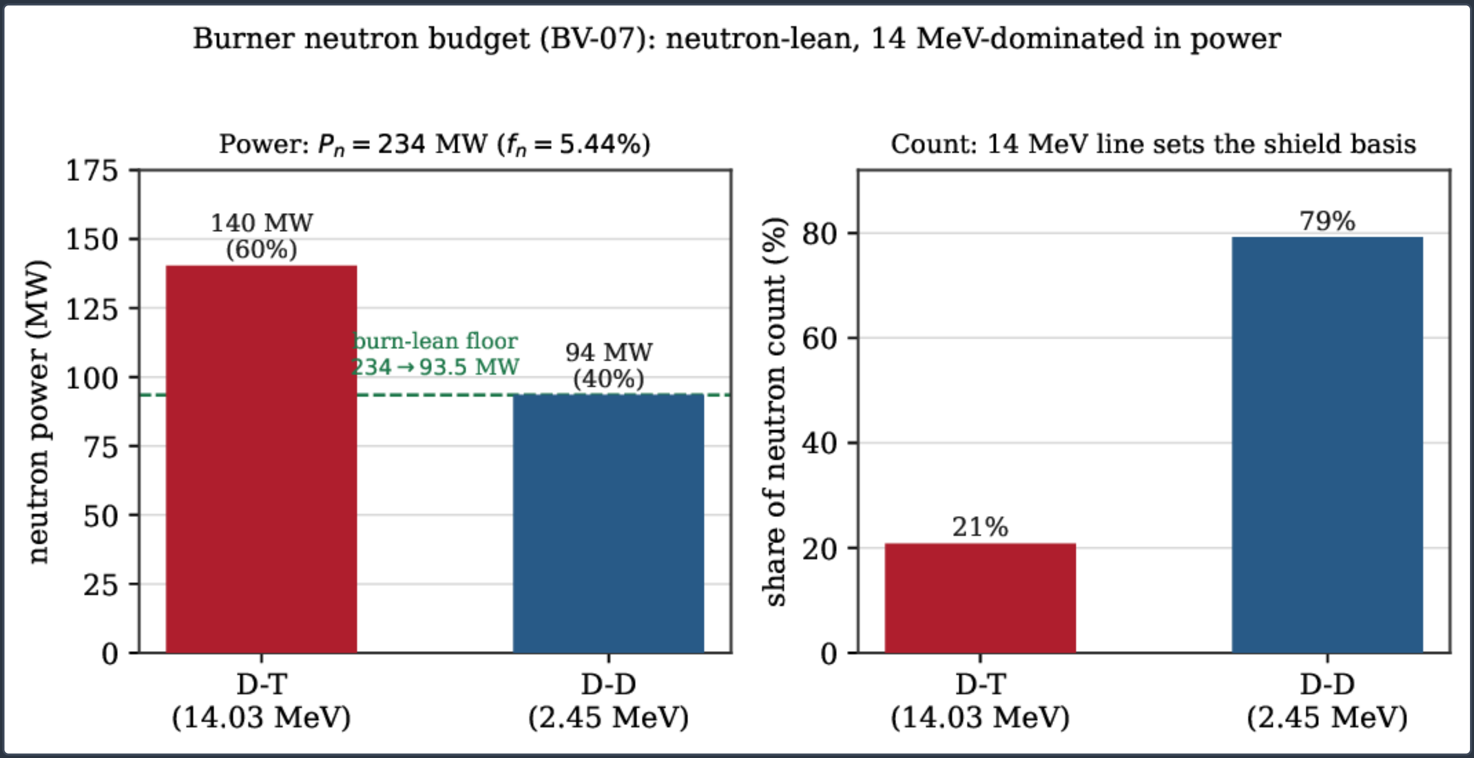

Burner neutron budget (BV-07). Left: neutron power splits 60/40 between the 14.03 MeV D–T self-burn and the 2.45 MeV D–D line; the burn-lean floor removes the hard line, dropping P_n from 234 to 93.5 MW. Right: by count the budget is dominated by the softer 2.45 MeV neutrons (79 %), yet the 14 MeV minority sets the shield basis. Both panels follow from the single burnup fraction $f_{\text{burn}} = 0.263$.

THE BURN-LEAN LEVER

Because the hard line is fed by a pumpable species, equation (11) is not merely descriptive but prescriptive: f_{burn} is a control variable, tuned through τ_p^* by the tritium pumping rate (AG-CX-16). Driving $f_{\text{burn}} \to 0$ takes the neutron power to the D–D floor,

$$P_n \longrightarrow P_{\text{DD}} = 93.5\ \text{MW} \qquad (\text{a } 60\,\% \text{ reduction}).$$

The fusion-power cost of doing so is small, because the D–T reactions removed are a thin slice of the total. The D–T fusion power is fixed by the hard-line neutron power through its Q-value,

$$\Delta P_{\text{fus}} = R_{DT} V\, Q_{\text{DT}} = P_n^{\text{DT}} \frac{Q_{\text{DT}}}{E_n^{\text{DT}}} = 140.4\ \text{MW} \times \frac{17.59}{14.03} = 176.0\ \text{MW},$$

so that

$$\frac{\Delta P_{\text{fus}}}{P_{\text{fus}}} = \frac{176.0}{4298.5} = 4.10\,\%, \qquad \frac{\Delta P_n}{P_n} = \frac{140.4}{233.95} = 60.0\,\%.$$

The ratio of these is a lever,

$$L \equiv \frac{\Delta P_n / P_n}{\Delta P_{\text{fus}} / P_{\text{fus}}} = \frac{60.0}{4.10} \approx 14.6,$$

so a plant can cut its neutron output by more than half for a few percent of gain (Figures 2, 3, 4). The same machine can therefore run neutron-richer where siting is permissive and burn-lean where it is not, trading in-situ tritium breeding for a softer radiation environment without a new build.

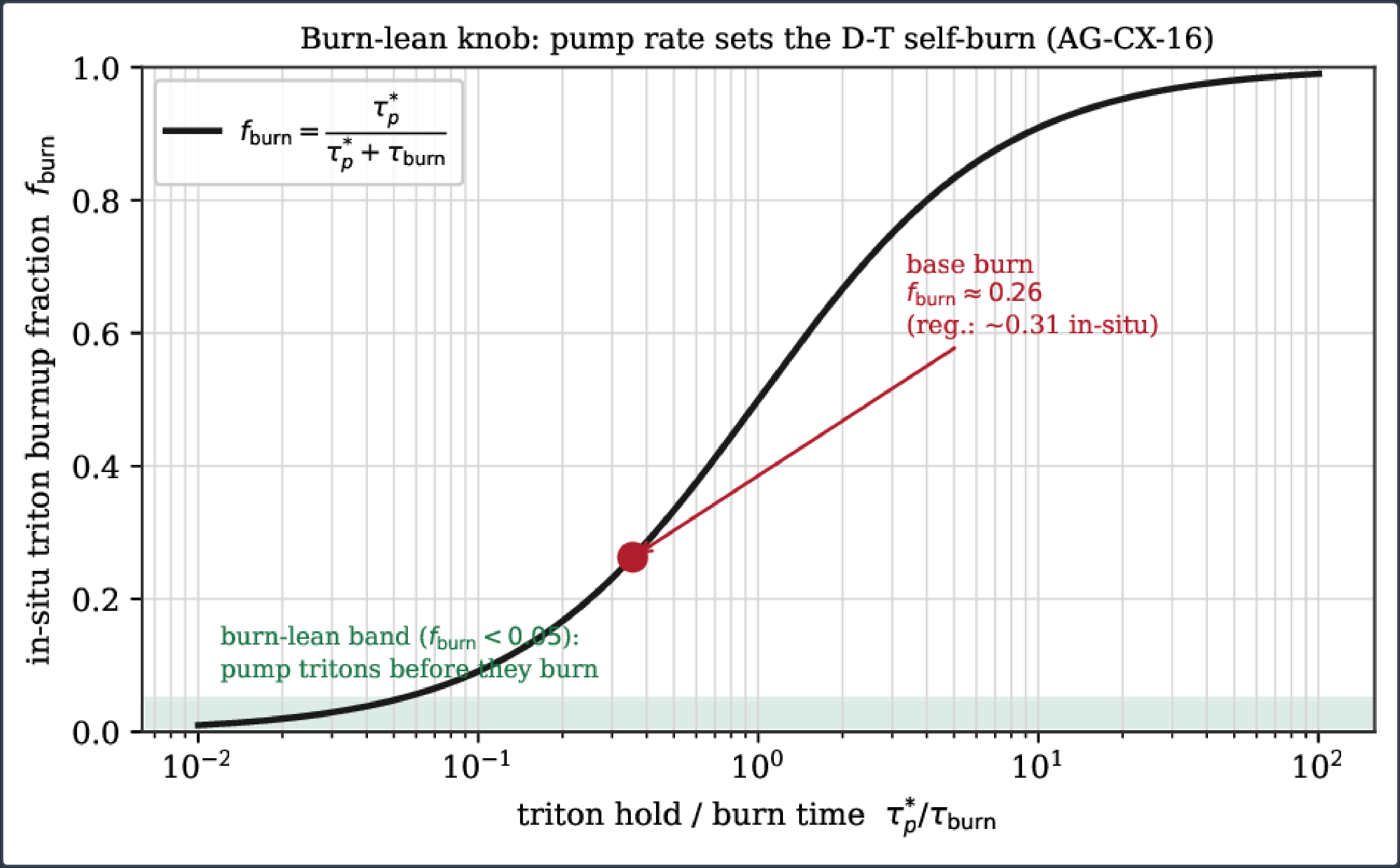

Triton burnup fraction, equation (7), as a function of the ratio of triton hold time to burn time. The design point sits at $f_{burn} \approx 0.26$ (red); driving the pump balance into the shaded band ($f_{burn} < 0.05$) is the burn-lean mode (AG-CX-16). The register's independent in-situ burn estimate (~ 0.31) is consistent within the D–D branching ratio.

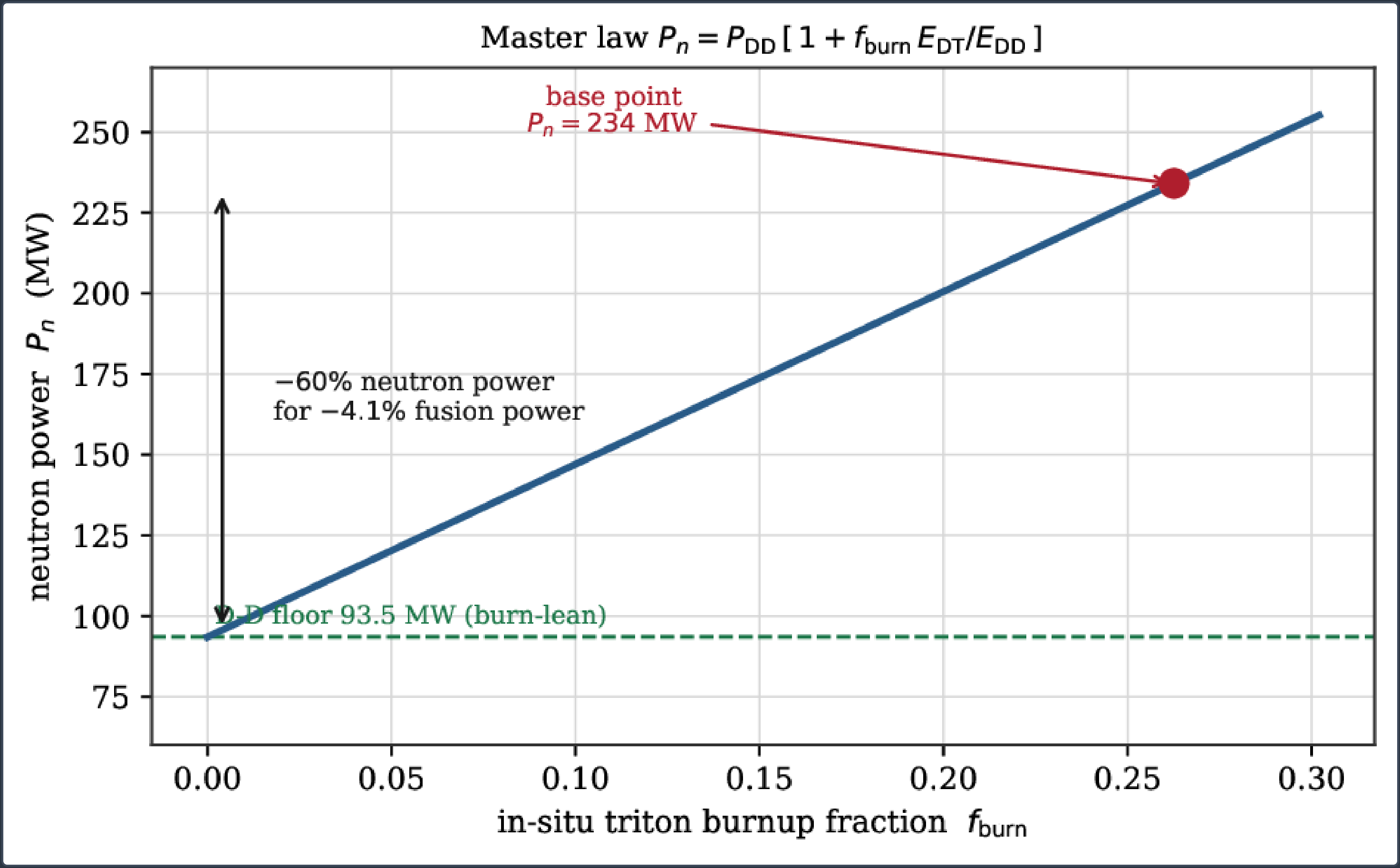

The master law (11): neutron power is linear in the burnup fraction, with intercept the 93.5 MW D–D floor (green) and slope $P_{DD}E_n^{DT}/E_n^{DD}$. The design point (red) is 234 MW at $f_{burn} = 0.263$; the burn-lean lever slides down this line to the floor.

§ 3

The operating point: radiation transport and closure

The neutron budget of §2 rests on a self-consistent plasma solution, not an assumed temperature. The central cell holds its ions against axial loss with an electrostatic ambipolar potential φ_i established in the end plugs; in a Pastukhov–Cohen picture the mirror-confined electron and ion end-loss fluxes balance to fix φ_i, with the confined-species loss scaling as [18,19,20]

$$(n\tau)_{\mathrm{end}} \;\propto\; g(R_{mc})\,\frac{\exp(\varphi_i/T_i)}{\varphi_i/T_i},$$

where R_{mc} is the mirror ratio and g a slowly varying geometric factor. At the design point $R_{mc} = 4.61$ and $\varphi_i = 248.75\,\mathrm{keV}$ with $\varphi_i/T_i = 2.764$, giving an ion temperature $T_i \simeq 90\,\mathrm{keV}$; the ambipolar and sloshing-ion physics that set this potential are developed in companion work [7,8] and are taken here as the fixed operating context.

The neutron rates in (4) depend on this temperature through the reactivities, so the budget is only as firm as the electron power balance that pins T_e. In a high-T_e, high-field mirror plasma the radiated channels are dominated by bremsstrahlung and synchrotron emission,

$$P_{\mathrm{heat,e}} = P_{\mathrm{brem}} + P_{\mathrm{sync}} + P_{\mathrm{end,e}}, \qquad P_{\mathrm{brem}} = C_B\,Z_{\mathrm{eff}}\,n_e^2\sqrt{T_e}, \quad P_{\mathrm{sync}} = C_S\,n_e T_e B^2\,\Phi(\mathcal{R}, T_e),$$

with $Z_{\mathrm{eff}} = 1.462$ and Φ the wall-reflectivity- and temperature-dependent synchrotron reabsorption factor. Synchrotron losses are model-sensitive in this regime, so the transport closure (KX-L1-A3-BU) carries *three* synchrotron models to bracket Φ; all three return the canonical anchors ($Q_E = 1.318$, $P_{\mathrm{fus}} = 4298.5\,\mathrm{MW}$, $P_n = 233.95\,\mathrm{MW}$, $f_n = 5.44\,\%$, $\varphi_i = 248.75\,\mathrm{keV}$) at a self-consistent electron temperature

$$T_e = 89.72\ \mathrm{keV} \quad (\text{maximum-}Q_E\ \text{mode}),$$

confirming the operating point is robust to the synchrotron uncertainty. The synchrotron-limited pinning of T_e and the recirculation-resolved Q_E closure are established at length in companion papers [6,9]; here they supply the temperature on which the reactivities, and hence the neutron budget, depend.

§ 4

Siting: shielding, dose and the tritium source term

Two quantities decide whether a source may sit near people and assets: the dose rate at the site boundary and the mobile radioactive inventory that an off-normal event could release. The neutron-lean cycle is favourable on both, and both admit compact, auditable models.

POINT-KERNEL DOSE FORMALISM

Treat the burner as an isotropic point source of strength S (fast neutrons, plus the secondary capture gammas they generate) behind a concrete slab of thickness t. The dose-equivalent rate at stand-off r is the attenuated, buildup-corrected point kernel [31,32]

$$\dot{D}(r,t) = \frac{S}{4\pi r^2}\, k_\Phi\, B(\mu t)\, e^{-\mu t},$$

where k_Φ is the fluence-to-dose-equivalent coefficient [33], μ the macroscopic removal coefficient of concrete and $B(\mu t)$ the dose buildup factor. Over the thick-slab range of interest the buildup and exponential combine to a near-exponential falloff, $B(\mu t)e^{-\mu t} \approx e^{-\mu_{\text{eff}} t}$, giving the working form

$$\dot{D}(r,t) = \dot{D}_0 \left(\frac{r_0}{r}\right)^2 e^{-\mu_{\text{eff}}(t-t_0)}.$$

THE EXPONENTIAL SHIELD LAW AND THE LOGARITHMIC PENALTY

Requiring $\dot{D} = \dot{D}_{\text{lim}} = 0.11\,\mu\text{Sv h}^{-1}$ at $r = 50$ m and solving (23) for the shield thickness gives

$$t = t_0 + \mu_{\text{eff}}^{-1} \ln\left(\frac{\dot{D}_0}{\dot{D}_{\text{lim}}}\right).$$

The point-kernel evaluation (MV-CX-28) returns $t_{\text{lean}} = 2.80$ m for the neutron-lean burner. For a D–T source of the *same* fusion power the source strength is larger by the neutron-fraction ratio $\rho = f_n^{\text{DT}}/f_n = 0.80/0.0544 = 14.7$, so its required thickness exceeds the burner's by

$$\Delta t = t_{\text{DT}} - t_{\text{lean}} = \mu_{\text{eff}}^{-1} \ln \rho,$$

which evaluates to $t_{\text{DT}} = 3.06$ m, a saving of only $\Delta t \simeq 0.26$ m (with $\mu_{\text{eff}} = \ln \rho/\Delta t \approx 0.103\ \text{cm}^{-1}$, a physical fast-neutron removal value for concrete; Figure 5). This is the paper's most easily misread result. *Shield thickness is only logarithmic in source strength*: a $14.7\times$ leaner source buys about a quarter of a metre of concrete, not a factor of fourteen. The operational value of neutron-leanness is therefore not the shield — it is the low *absolute* loading, $0.098\ \text{MW m}^{-2}$, which is what keeps activation, occupied-area dose, and the consequence of a shield imperfection low enough to matter for a sited plant (Figure 6).

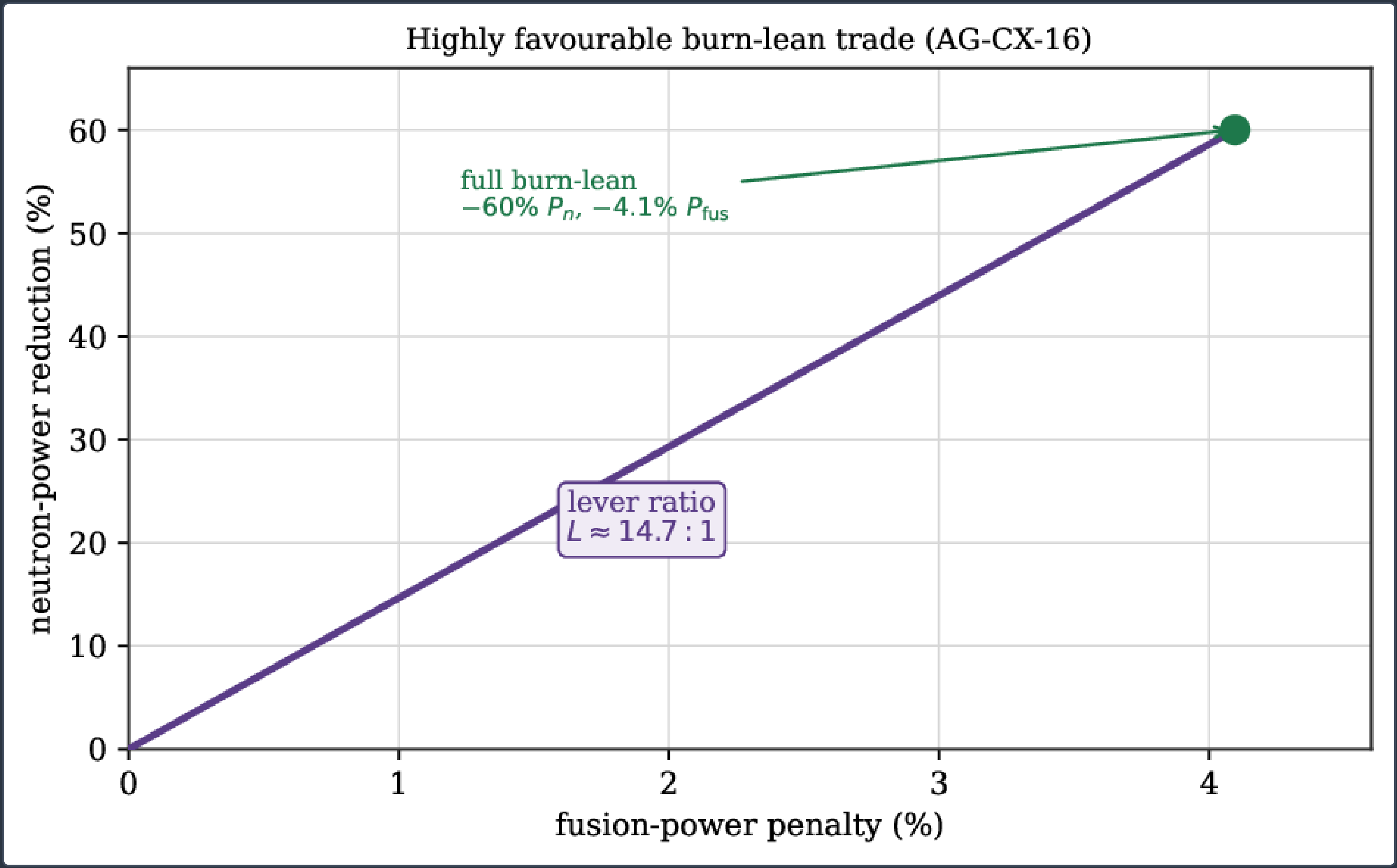

The burn-lean trade (AG-CX-16): neutron-power reduction against fusion-power penalty as the D–T self-burn is progressively pumped out. Full burn-lean removes 60 % of P_n for a 4.1 % fusion-power penalty — a 14.6:1 lever, equation (18).

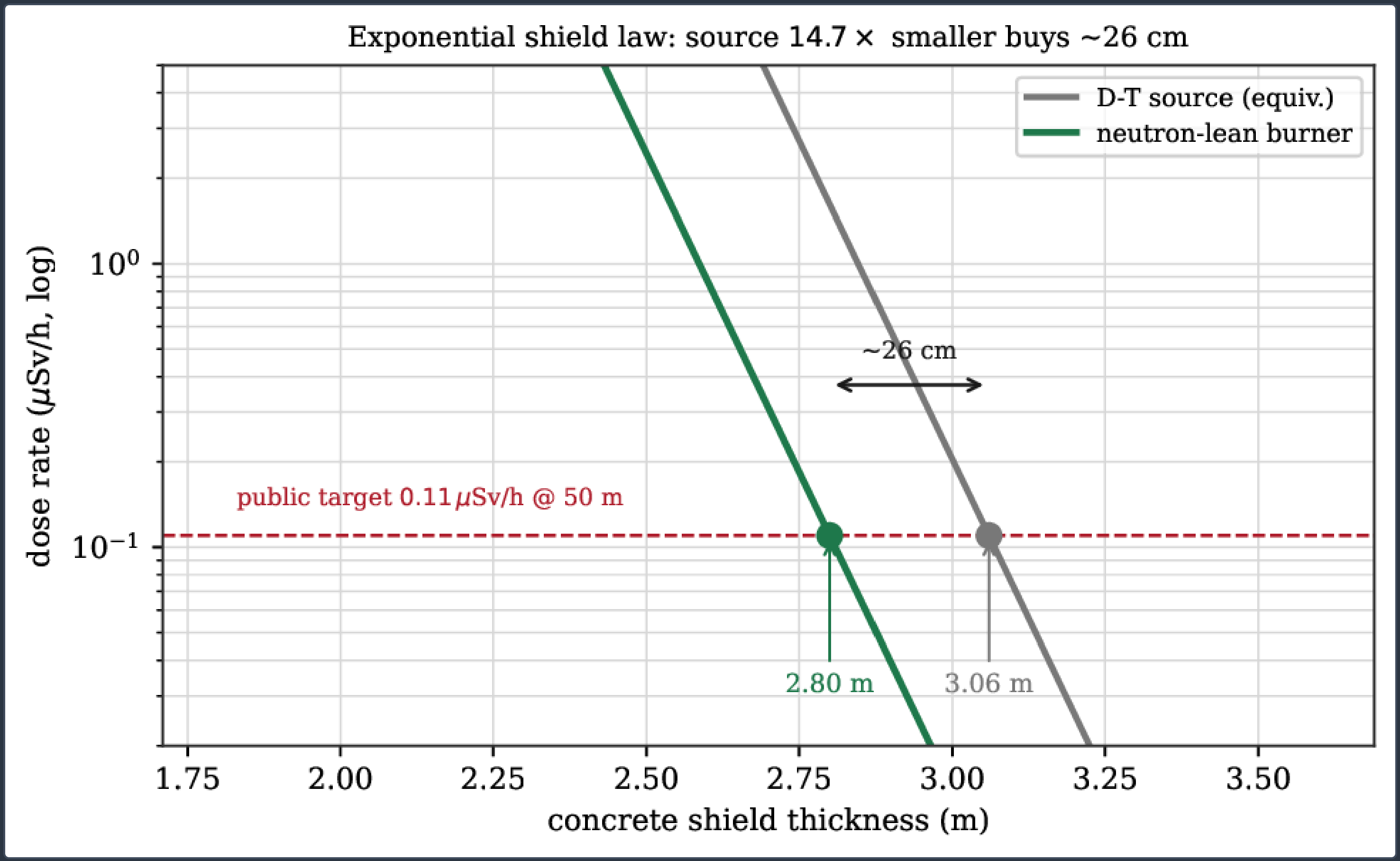

Point-kernel dose versus concrete thickness (MV-CX-28), equation (23), for the neutron-lean burner (green) and a same-power D–T source (grey). Both meet the $0.11\,\mu\mathrm{Sv\,h}^{-1}$ public target at 50 m, but the $14.7\times$ leaner source saves only ~ 26 cm — the logarithmic penalty of equation (25). Note the logarithmic dose axis.

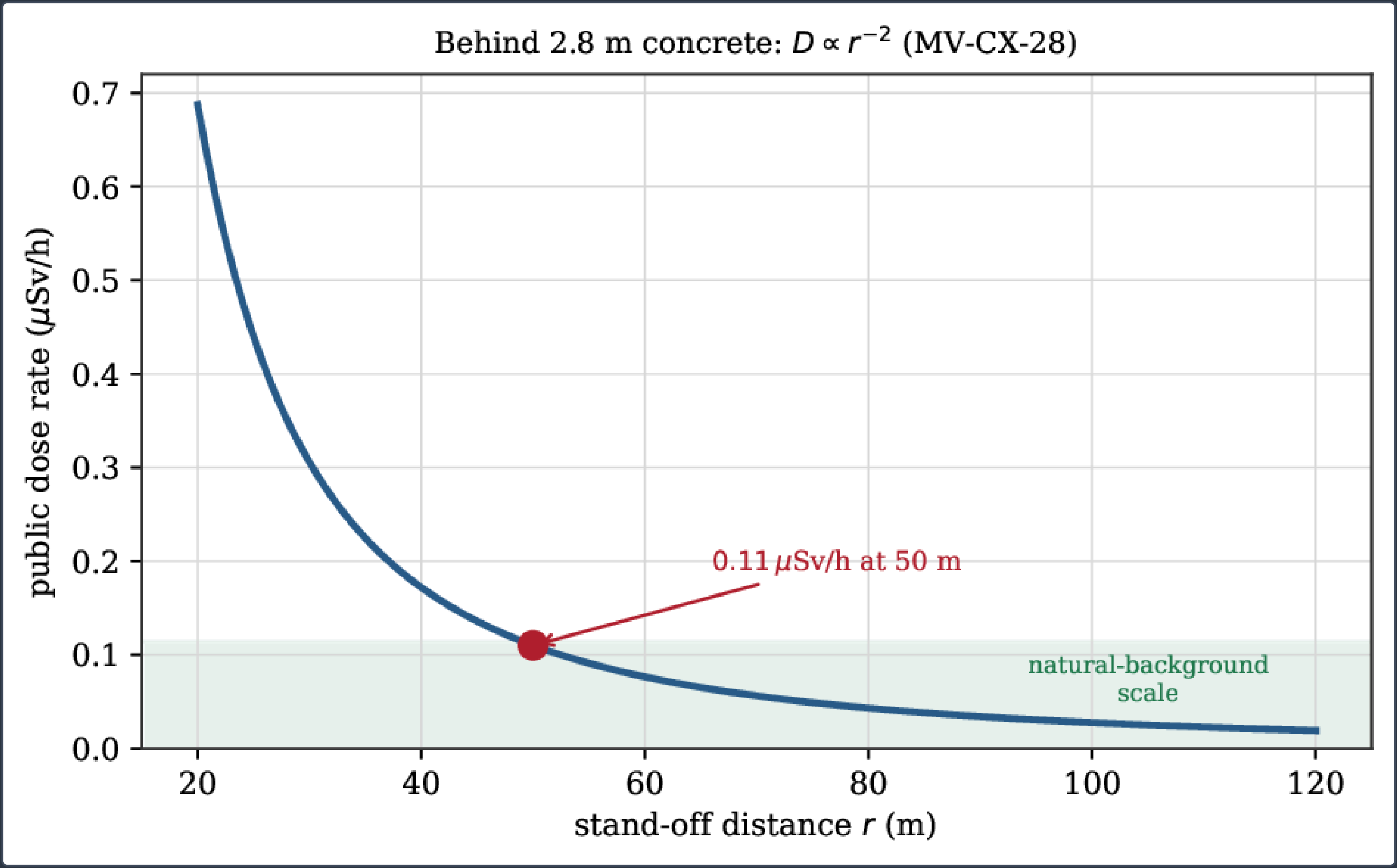

Public dose rate versus stand-off distance behind the buildable **2.80** m concrete shield (MV-CX-28), $\dot{D} \propto r^{-2}$ from equation (23). The design meets **0.11** μSv h^{-1} at **50** m (red), falling into the natural-background band beyond it.

THE MOBILE TRITIUM SOURCE TERM

The larger siting advantage is on tritium, and here the relevant quantity is subtle. The burner's predominantly aneutronic cycle self-generates about 32 kg of tritium per full-power year through the D–D triton branch (2) and burns a fraction $f_{\text{burn}} \approx 0.31$ of it in situ (MV-CX-29). But total generation is not the licensing basis; the licensing basis is the *mobile* inventory — the tritium that is in a releasable form (gas-phase, in the fuel-handling loop) at any instant. Modelling the mobile loop as a well-mixed buffer with net tritium throughput $\dot{N}_T$ and processing residence time τ_{hold},

$$I_{\text{mob}} = \dot{N}_T\, \tau_{\text{hold}}, \qquad \dot{N}_T = \frac{32\ \text{kg fpy}^{-1}}{3.156 \times 10^7\ \text{s fpy}^{-1}} = 1.01 \times 10^{-3}\ \text{g s}^{-1},$$

so a one-hour hold gives

$$I_{\text{mob}} = 1.01 \times 10^{-3}\ \text{g s}^{-1} \times 3600\ \text{s} = 3.6\ \text{g}.$$

Against the ~ 1 kg mobile inventory characteristic of a D–T-class plant, this is a source term $\sim 275\times$ smaller (Figure 7), and it is the single strongest argument for placing the burner near the load it serves. The self-generated tritium is itself a strategic co-product feeding the breeder–burner fuel architecture [5], but it does not enlarge the mobile inventory that a permit turns on.

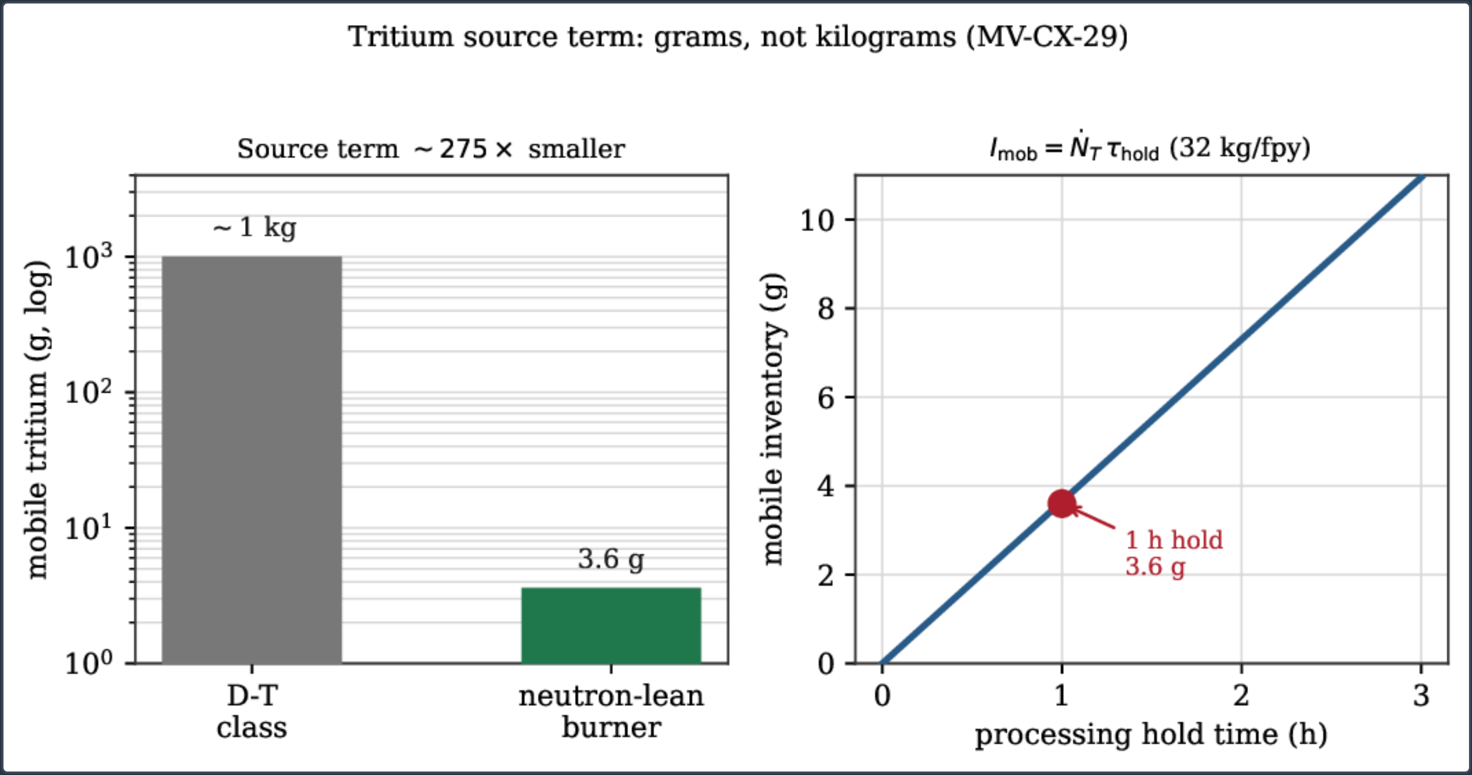

Mobile tritium source term (MV-CX-29). Left: mobile inventory ~ 3.6 g versus ~ 1 kg for a D–T-class plant, $\sim 275\times$ smaller (log axis). Right: the residence-time model of equation (26)–(27); a one-hour processing hold at 32 kg fpy^{-1} throughput yields 3.6 g.

§ 5

Computational methodology: the GPU HPC campaign

Every number in §2–§4 was produced and cross-checked on the Kronos NVIDIA GPU HPC campaign, run on a mixed A100/H100/A10 fleet. Four codes carry the work, each accelerated on the GPU fleet and each tied to a frozen register serial.

Mirror power-balance and radiation transport. The KRONOS Toolkit mirror solver (`solve_mirror`) integrates the coupled 0-D power balance (20) with the ambipolar closure (19) and the three synchrotron models, sweeping the operating plane to locate the maximum-Q_E mode (KX-L1-A3-BU). Because the closure is a low-dimensional but stiff root-find repeated over a large design grid, the campaign batches thousands of independent operating-point solves across GPU threads, returning the self-consistent $T_e = 89.72$ keV (21) and the frozen anchors. The neutron split of (11) and the triton kinetics of (7) are evaluated on the same reactivity tables [12].

Monte-Carlo neutron and photon transport. The three-dimensional transport that underlies the shield and activation basis is carried by OpenMC with ENDF/B-VIII.0 evaluated nuclear data [26,27]. OpenMC's history-based Monte Carlo is embarrassingly parallel and is run on the GPU fleet for the deep-penetration dose problem; because the sited dose is a rare-event, deep-shield tally, the campaign uses weight-window variance reduction to drive the tally variance down at fixed wall-clock. The point-kernel results reported here (MV-CX-28) are the fast basis; the converged 3-D Monte-Carlo activation and dose maps for the actual housing geometry — with ducts, penetrations and the capture-gamma field outside the 1–3 m shield — are set up on the identical source term as the confirming step (BV-08 activation and dose; AG-CX-15 defense-housing dose).

Point-kernel dose and inventory. The dose kernel (22) and the mobile-tritium model (26) are lightweight analytic reductions evaluated directly against the transport source strength; they are cheap enough to run inside a design sweep and are the basis-level tools that the Monte-Carlo runs confirm.

Verification and reproducibility. The campaign reproduces the registered burner anchors byte-for-byte across independent re-runs: $Q_E = 1.318$, $P_{\mathrm{fus}} = 4298.5$ MW, $P_n = 233.95$ MW, $f_n = 5.443\,\%$, $\varphi_i = 248.75$ keV, $T_e = 89.72$ keV. The derived quantities of this paper close on those anchors to the digit: the wall loading (14) returns 0.0984 MW m^{-2}, the master law (11) returns 234.1 MW at $f_{\mathrm{burn}} = 0.263$, the burn-lean penalty (17) returns $4.10\,\%$, the lever (18) returns $14.7{:}1$, and the mobile-tritium model (27) returns 3.65 g. The figure-generation script is archived with the deposit and regenerates every panel from these frozen inputs.

§ 6

Results

Table 2 collects the resolved budget, the operating point, the burn-lean lever and the siting margins. The results are internally consistent by construction — the count and power splits, the wall loading, and the burn-lean trade all descend from the single burnup fraction $f_{\text{burn}} = 0.263$ and the two frozen anchors $P_n = 233.95$ MW and $P_{\text{DD}} = 93.5$ MW — so the budget cannot be internally contradicted without moving an anchor.

QUANTITY	SYMBOL	VALUE	SERIAL
fusion power	P_{fus}	4298.5 MW	M-45
neutron power	P_n	233.95 MW	BV-07
neutron fraction	f_n	5.44 %	BV-07
wall neutron loading	Γ_n	0.098 MW m^{-2}	BV-07
hard-line power / count	—	60 % / 21 %	BV-07
soft-line power / count	—	40 % / 79 %	BV-07
in-situ triton burnup	f_{burn}	0.26–0.31	MV-CX-29
self-consistent T_e	T_e	89.72 keV	KX-L1-A3-BU
ambipolar potential	φ_i	248.75 keV	KX-L1-A3-BU
burn-lean floor	P_n^{min}	93.5 MW	AG-CX-16
burn-lean neutron cut	$\Delta P_n/P_n$	60 %	AG-CX-16
burn-lean fusion penalty	$\Delta P_{\text{fus}}/P_{\text{fus}}$	4.1 %	AG-CX-16
lever ratio	L	14.6:1	AG-CX-16
urban shield (public dose)	t_{lean}	2.80 m concrete	MV-CX-28
D–T equivalent shield	t_{DT}	3.06 m concrete	MV-CX-28
public dose at 50 m	$\dot{D}$	0.11 μSv h^{-1}	MV-CX-28
mobile tritium inventory	I_{mob}	3.6 g	MV-CX-29
source-term ratio to D–T	—	$\sim$275× smaller	MV-CX-29

Resolved neutron-lean siting summary for the Kronos D–^{3}He burner. Serials refer to the Kronos Physics De-Risking Register [1].

Figure 8 places the burner against the benchmark classes. Its neutron fraction, 5.44 %, is 14.7× below the $\sim$80 % of a D–T plant and sits between the ideal aneutronic limit (zero, all neutrons parasitic) and the D–T regime; its wall neutron loading, 0.098 MW m^{-2}, is one to two orders below the first-wall loadings of ITER-class and ARC-class D–T devices. The two-housing conclusion of §7 is summarised schematically in Figure 9.

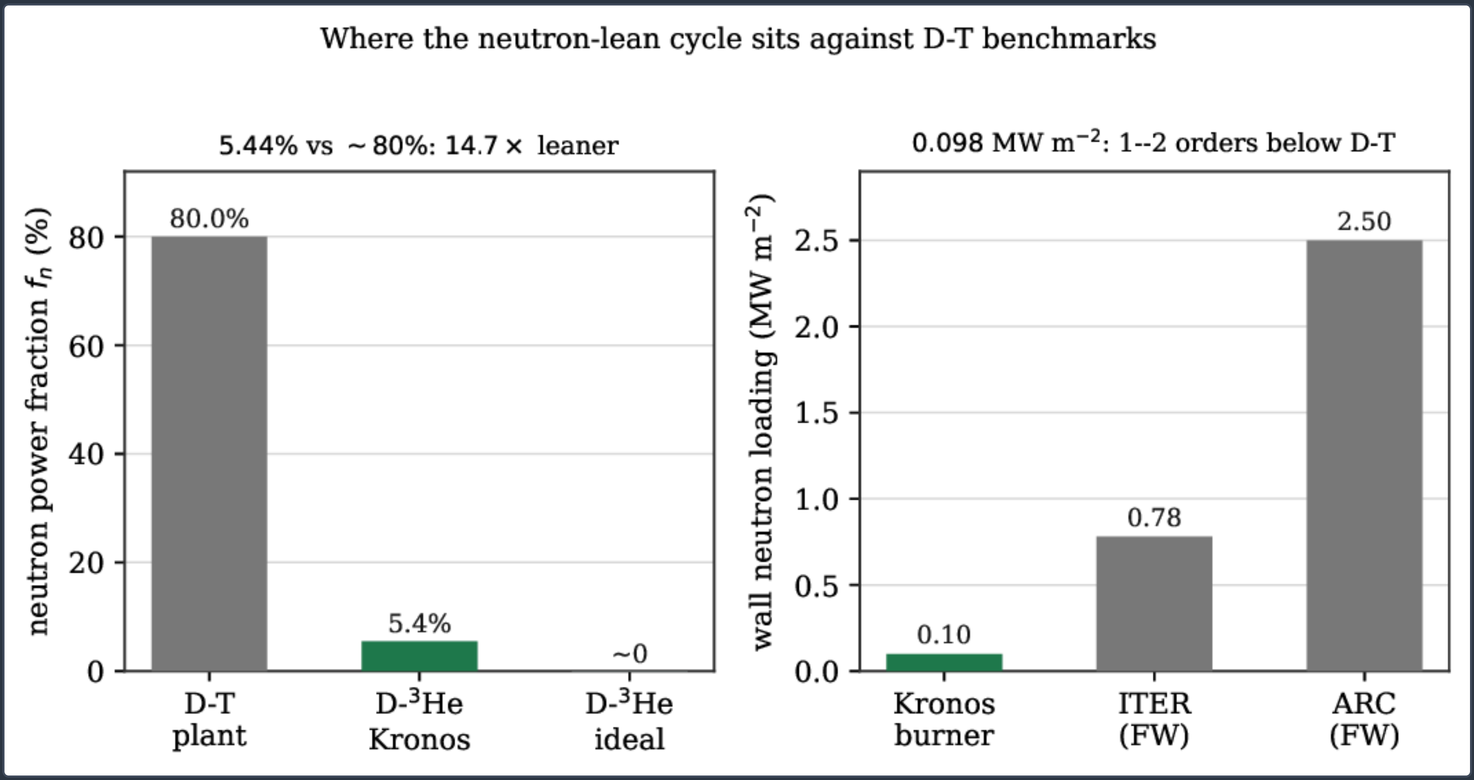

The neutron-lean cycle against D–T benchmarks. Left: neutron power fraction f_n — $5.44\,\%$ for the Kronos burner versus $\sim 80\,\%$ for a D–T plant, $14.7\times$ leaner, with the ideal (parasitic-only) limit at zero. Right: wall neutron loading — 0.098 MW m^{-2} against representative ITER and ARC first-wall class values.

§ 7

Two housings: fixed-defense and urban

The same neutron-lean source underwrites two deployment configurations that differ only in what they most value in it. A *fixed-defense* installation (Aegis) values the low activation, small footprint and gram-scale mobile inventory for a compact, defensible, islanded plant [2]; an *urban*, demand-adjacent unit (MetroVolt) values the same properties for a public-facing permit near the load it powers [3]. Both inherit the budget, operating point and source term established here, and both carry a dedicated, higher-fidelity dose and activation map as the confirming analysis — the defense-housing dose (AG-CX-15) and the activation and dose field outside the **1–3** m shield (BV-08) — set up as full Monte-Carlo transport runs on the point-kernel basis of this paper. The burn-lean lever (18) is available to both: a housing can dial its neutron output to the D–D floor where its siting is most constrained.

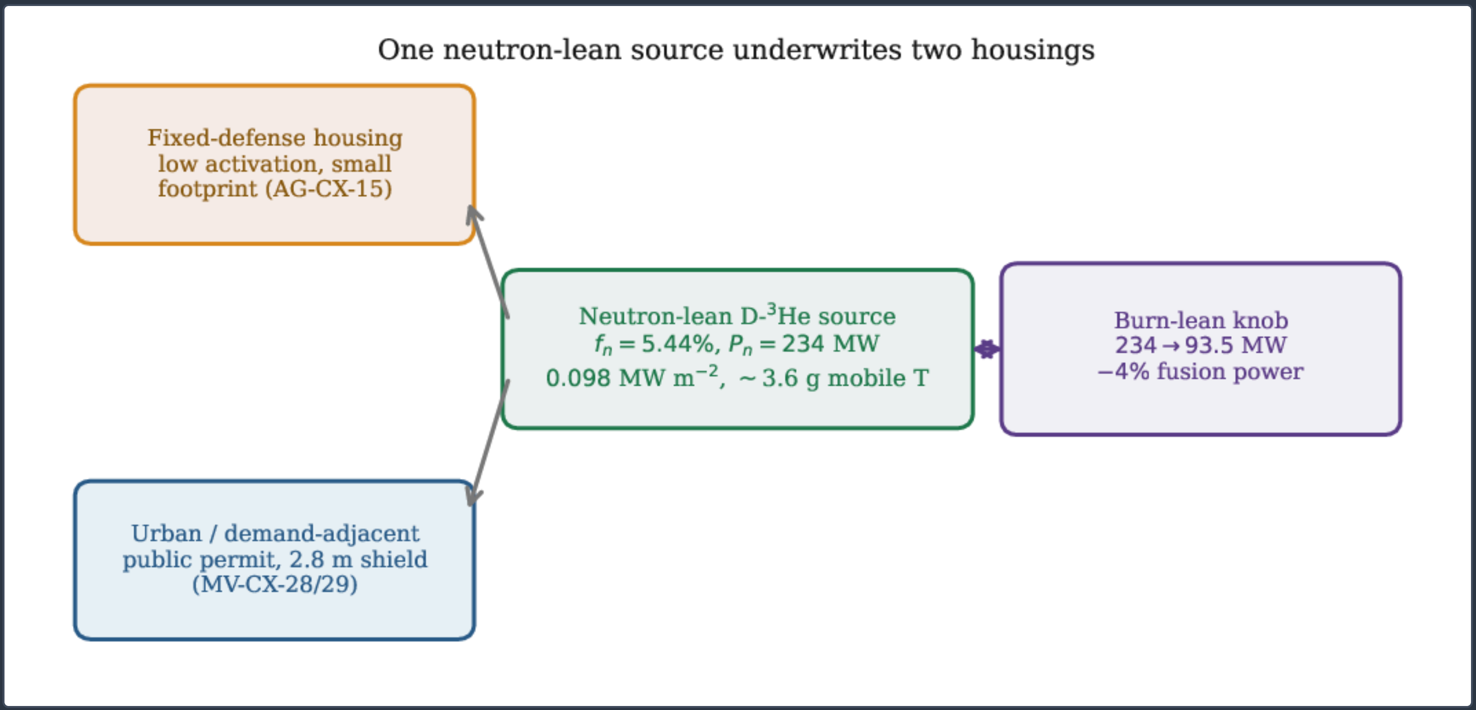

(Schematic.) One neutron-lean source underwrites two housings. The common source ($f_n = 5.44\,\%$, $P_n = 234$ MW, 0.098 MW m^{-2}, ~ 3.6 g mobile tritium) feeds a fixed-defense housing (AG-CX-15) and an urban housing (MV-CX-28/29); the burn-lean knob slides the neutron output to the **93.5** MW D–D floor. No data values are computed in this figure; it encodes structure only.

§ 8

Discussion

The burner's neutronics *are* its siting case, and the analysis makes each step quantitative and comparable to the published literature. A neutron fraction of $5.44\,\%$ and a sub-$0.1\,\mathrm{MW\,m^{-2}}$ wall loading place the machine in a different class from a D–T source: ITER's first wall is designed for ~ 0.5–$0.8\,\mathrm{MW\,m^{-2}}$ of 14 MeV loading and ARC-class pilots for $\sim 2.5\,\mathrm{MW\,m^{-2}}$ [36,35], so the burner's $0.098\,\mathrm{MW\,m^{-2}}$ is five to twenty-five times lower — the reason its activation and remote-handling burden collapse. Resolving the budget by energy line, rather than reporting a scalar flux, identifies the 14 MeV D–T self-burn as the shield- and damage-setting term even though it is the minority by count; this is the kind of structure a lumped "neutron output" number hides, and it is what the burn-lean lever acts on directly.

The two levers convert that physics into deployability. The burn-lean trade, equation (17)–(18), is favourable precisely because the hard line is a small *fusion*-power term (a 17.59 MeV reaction supplying 176 MW of a 4298.5 MW total) but a large *neutron*-power term ($60\,\%$ of P_n); the $14.6{:}1$ lever is a direct consequence of that asymmetry and of the pumpability of tritium. The tritium source term is the stronger siting argument: a mobile inventory of grams rather than kilograms changes the accident source term, the emergency-planning basis, and the proliferation-relevant special-nuclear-material picture by more than two orders of magnitude [34,29], which is why the byproduct-material licensing pathway is available to the burner as it is to the breeder [11,10]. Where the analysis is deliberately conservative is the shield: because attenuation is exponential, the $14.7\times$ leaner source buys only ~ 26 cm of concrete (equation (25)), so we do *not* claim shield thickness as the advantage — the advantage is the low absolute loading and the small mobile inventory, both of which are genuine and large.

§ 9

Limitations

The dose and shield numbers reported here are point-kernel calculations with the buildup factor folded into an effective attenuation coefficient (equation (23)); this is a sound *basis* for the source term and the shield scaling, but it does not resolve the capture-gamma field, duct and penetration streaming, or skyshine for a specific housing geometry. Those require the converged **3**-D Monte-Carlo transport runs (BV-08, AG-CX-15), which are set up on the identical source term but are not yet run to statistical convergence; they are the confirming step, and until they close, the housing-specific dose maps should be read as provisional. This is the single honest gate on the siting case; the neutron budget itself (§2), being tied to the frozen operating point, is not subject to it.

§ 10

Conclusion

The Kronos burner is neutron-lean: $f_n = 5.44\,\%$, $P_n = 233.95$ MW, and a wall loading of 0.098 MW m^{-2}. Its neutron budget resolves into a hard 14.03 MeV D–T self-burn line carrying $60\,\%$ of the power but $21\,\%$ of the count — the shield-setting term — and a soft 2.45 MeV D–D line carrying the rest, both following from a single triton burnup fraction $f_{\mathrm{burn}} \approx 0.26$. A self-consistent radiation-transport solution fixes the operating point at $T_e = 89.72$ keV. A burn-lean mode cuts the neutron power to the 93.5 MW D–D floor for a $4.1\,\%$ fusion-power penalty, a 14.6:1 lever; and the predominantly aneutronic cycle holds a mobile tritium inventory $\sim 275\times$ smaller than a D–T plant, giving a public dose of $\sim 0.11\,\mu$Sv h^{-1} at 50 m behind 2.80 m of concrete. A machine that can be shielded to background-scale dose and holds grams, not kilograms, of mobile tritium is a machine that can be sited near people and assets — for both a fixed-defense and an urban housing.

Acknowledgments tocsectionAcknowledgments Part of the Kronos Fusion Energy 2026 design series. The authors thank the Kronos de-risking team for the frozen register serials on which this analysis is built.

Reproducibility. The neutron budget, radiation-transport operating point, burn-lean trade, shield curve and tritium source term are frozen anchors (BV-07, KX-L1-A3-BU, AG-CX-16, MV-CX-28, MV-CX-29) in the Kronos Physics De-Risking Register and are regenerable from the neutron-split, triton-kinetics, point-kernel and inventory scripts archived with this paper. This paper is archived at its DOI doi:10.5281/zenodo.22645917 and its official page https://www.kronosfusionenergy.com/publications/the-neutron-lean-siting-case-for-a-d-he-tandem-mirror-b.html; the de-risking register is archived at doi:10.5281/zenodo.22133057.

Data availability tocsectionData availability This paper is archived at doi:10.5281/zenodo.22645917. The neutron-budget arrays, the radiation-transport outputs, the shield curve and the tritium-inventory calculation are archived with the deposit and reference the Kronos 2026 series. Any economic analysis is reported separately and is not included in the public deposit.

Competing interests tocsectionCompeting interests Provisional patent applications relating to aspects of this work have been filed. The authors declare no other competing interests.

APPARATUS

Portfolio, People & Record

The intellectual-property estate, the people who built it, the limitations that gate it, and the sources it rests on.

1	4	40	27
GRANTED PATENT	2026 PROVISIONALS	TEAM MEMBERS	2022 PROVISIONALS

INTELLECTUAL PROPERTY

The patent portfolio

The estate spans a granted high-field magnet patent, pending utility and 2026 provisional filings that map to the two products, a digital-twin control provisional, a registered trademark application, and the original 2022 provisional family. Every patentable disclosure in the five-paper arXiv drop was protected **before** publication: the breeder and burner provisionals were filed 1–2 August, and a publication-gap omnibus filing the evening before the drop swept up the DEC, plasma-control, and REBCO-winding matter of the three otherwise-unprotected papers. Patent numbers and application serials are matters of public record; claim scope is summarised, not reproduced.

GRANTED & PENDING UTILITY

US 12,009,112	High-field tilted graded-REBCO magnet architecture (KRONO-002A) · *app. 17/878,550*	GRANTED
US 17/878,507	Core device / method (KRONO-001A) · *utility*	PENDING

2026 PROVISIONAL FILINGS — MAPPED TO THE PRODUCTS

64/124,209	Hyperion — spherical-tokamak tritium / helium-3 foundry · *breeder · filed Aug 2026*	FILED
64/124,220	Aegis / MetroVolt — synchrotron-cutoff, fuel-selection & plug-winding · *generator · filed Aug 2026*	FILED
64/115,167	KRONOS-CTRL digital-twin plant control · *provisional · filed Jul 2026*	FILED
64/005,440	Integrated spherical-tokamak fusion architecture · *early integrated-architecture filing · filed Mar 2026*	FILED
64/105,530	Negative-triangularity spherical-tokamak architecture · *foundational ST filing · filed Jul 2026*	FILED
64/128,097	Publication-gap omnibus — quasineutral two-species expander DEC · provenance-gated / latency-split plasma control · as-built high-field winding & conductor architecture · *filed 7 Aug 2026, the evening before the arXiv drop*	FILED

TRADEMARK & ORIGIN

FTK-98801894	Kronos Fusion Energy — trademark application	FILED
KR-2022-*	Original provisional family (KR-2022-00001 … 00027) · *27 filings, 2022*	PRIORITY

The narrow, defensible magnet novelty — the specific conductor and the digital-twin winding optimisation, not high-field REBCO as a category — is the commercial core that can earn ahead of any Q > 1 milestone, with markets in fusion magnet supply, MRI/NMR, accelerators, and proton therapy. The claim is scoped honestly: the high field is a *system field* result, not a stand-alone-coil record; the small-bore plug coil is structurally infeasible as a bare winding but resolved by a stress-managed structural shield (feasible-pending-FEA); and the winding-tape experiment returned a *null result*. The value is the method, not a field record.

THE TEAM

Founding partners, board, advisors & auditors

Kronos is built by a bench of advanced-fuel-fusion, high-field-magnet, direct-conversion, and materials specialists, with a board and operations team drawn from defense, national laboratories, and industry. Dates are shown as ranges; where a tenure has ended or is term-ending, the range says so.

FOUNDING PARTNERS — SCIENCE

Dr. Gerald Kulcinski
Co-Founder · Helium-3 & Advanced-Fuel Fusion
UW–Madison · 2023–Present

Dr. Carl Weggel
Chief Scientist / S.M.A.R.T. Design
MIT Alcator Program · 2022–Present

Dr. Robert J. Weggel
Magnetic Field Design
MIT Magnet Lab · 2022–Present

BOARD

Priyanca Ford
Founder & CEO · Executive Board
2022–Present

Bandel Carano
Finance / Strategy
Oak Investment Partners / Stanford · 2025–2026

Patrick Schweiger
Fusion Device Engineering
Oklo / CFS / TerraPower · 2025–Present

SCIENTIFIC ADVISORS

Dr. Steven O. Dean
Fusion Policy & History
DOE / Fusion Power Associates · 2025–Present

Dr. Patrick H. Diamond
Plasma Turbulence & Transport
UC San Diego · 2025–Present

Dr. Jack J. Dongarra
HPC & Numerical Algorithms
Turing Award · 2025–Present

Dr. Nasr M. Ghoniem
Chief Material Scientist
UCLA · 2025–Present

Dr. Siegfried Glenzer
Plasma Physics & Laser Fusion
Stanford / SLAC · 2022–Present

Dr. David A. Hammer
Pulsed-Power Fusion
Cornell · 2025–Present

Dr. Donald A. Spong
Plasma Theory & Confinement
ORNL · 2025–Present

Dr. Curtis Smith
Risk Assessment & Nuclear PRA
MIT / Idaho National Lab · 2025–Present

RADM (Ret.) David Goggins
Naval Engineering & Power-Plant Design
U.S. Navy · 2023–2026

Dr. Konstantin Batygin
Mathematician
Caltech · 2022–2025

Dr. Ruben Fair
Magnet Design / ITER Liaison
PPPL / Jefferson Lab · 2022–2025

Dr. Paul S. Weiss
Materials & Nanotechnology
UCLA · 2022–2025

SCIENTIFIC AUDITORS

Dr. Wilfred A. Cooper
Plasma Equilibrium Theory
EPFL / Swiss Plasma Center · 2025–Present

Dr. Ahmed Hassanein
Plasma–Material Interactions
Purdue / Argonne · 2025–Present

Dr. Patrick E. Hopkins
Extreme Thermal Materials
U. of Virginia · 2025–Present

Dr. Peter Hosemann
Materials Joining & Structural Integrity
UC Berkeley · 2025–Present

Dr. Travis W. Knight
Advanced Nuclear Fuels & Systems
U. of South Carolina · 2025–Present

Dr. Philippe Lebrun
Cryogenics & Magnet Cooling
CERN · 2025–Present

Dr. Nitendra Singh
Nuclear Safety & Fuel Cycle
ITER · 2025–Present

Dr. Guido Van Oost
Magnetic Confinement & Fusion Systems
Ghent University · 2025–Present

Dr. Gary S. Was
Radiation Materials & Structural Integrity
U. of Michigan · 2025–Present

Dr. Ray Sedwick
Direct Energy Conversion
U. of Maryland · 2025

OPERATIONS

Michael Laughlin
Chief Operating Officer
2022–Present

Martin Owens
Chief Strategy Officer
LANL / GE Hitachi · 2022–Present

MG (Ret.) Paul Pardew
Chief Contracting Officer
Army Contracting Command · 2022–Present

David Beck
Fusion Commercialization
U.S. Space Force · 2024–Present

Sushma Bhatia
Environmental & Legislative
Google · 2022–Present

Michael De Frenza
Technology Licensing
2023–Present

MG (Ret.) Robin L. Fontes
Cybersecurity & Defense
Army Cyber Command · 2022–Present

Vijay Gehani
Supply Chain & Components
INOX India · 2024–Present

Jon Michel Greenwood
IT & AI Infrastructure
Live Nation · 2023–Present

Brian C. O'Neill
National Security
CIA / ODNI · 2022–Present

Gen. (Ret.) Gustave F. Perna
DoD Liaison
Operation Warp Speed · 2022–2023

Andrea Romero
Marketing Lead
2022–Present

Legal counsel is retained; those roles are held on the internal roster and are not listed here.

SOURCES

References

1 P I Ford, *Kronos Physics De-Risking Register*, Kronos Fusion Energy 2026 series, doi:10.5281/zenodo.22133057.

2 P I Ford and G L Kulcinski, *The Aegis Forward-Base Burner: Q_E Closure, Plug Requirement, and Mirror Confinement in an Islanded Low-Neutron D–^{3}He Tandem Mirror*, Kronos series 1.2a, doi:10.5281/zenodo.22645693. https://www.kronosfusionenergy.com/publications/aegis-burner.html

3 P I Ford and G L Kulcinski, *The MetroVolt Data-Center Burner: Direct-DC Campus Power, Q_E Closure, and the Plug Requirement in a Low-Neutron D–^{3}He Tandem Mirror*, Kronos series 1.2b, doi:10.5281/zenodo.22645695. https://www.kronosfusionenergy.com/publications/metrovolt-burner.html

4 P I Ford, *An Advanced-Fuel Scorecard for D–T, D–D, D–^{3}He and p–^{11}B: Reactivity, Neutron Fraction and Direct-Conversion Trades*, Kronos series 2.2, doi:10.5281/zenodo.22645766. https://www.kronosfusionenergy.com/publications/advanced-fuel-scorecard.html

5 P I Ford and G L Kulcinski, *The D–^{3}He Fuel Cycle Does Not Close Indigenously: Helium-3 Supply, the Lunar Gate, and the Breeder's Strategic Co-Product*, Kronos series 2.35, doi:10.5281/zenodo.22645734. https://www.kronosfusionenergy.com/publications/helium-3-fuel-cycle.html

6 P I Ford and G L Kulcinski, *Synchrotron Radiation Transport in a D–^{3}He Tandem-Mirror Burner: Pinning the Electron Temperature at the Maximum-Q_E Operating Point*, Kronos series 2.55, doi:10.5281/zenodo.22645772. https://www.kronosfusionenergy.com/publications/synchrotron-radiation-transport.html

7 P I Ford and G L Kulcinski, *ECH-Sustained Thermal-Barrier Decoupling in the D–^{3}He Tandem-Mirror Plug*, Kronos series 2.56, doi:10.5281/zenodo.22645781. https://www.kronosfusionenergy.com/publications/ech-thermal-barrier-decoupling.html

8 P I Ford and G L Kulcinski, *Sloshing-Ion Ambipolar-Potential Formation in a D–^{3}He Tandem-Mirror Burner*, Kronos series 2.57, doi:10.5281/zenodo.22645913. https://www.kronosfusionenergy.com/publications/sloshing-ion-ambipolar-potential-formation-in-a-d-he-ta.html

9 P I Ford and G L Kulcinski, *Recirculation-Resolved Q_E Closure in a D–^{3}He Tandem-Mirror Burner: The Synchrotron-Limited Operating Point and the Carried-Open Plug Gate*, Kronos series 2.61, doi:10.5281/zenodo.22645860. https://www.kronosfusionenergy.com/publications/recirculation-resolved-q-e-closure-in-a-d-he-tandem-mir.html

10 P I Ford and G L Kulcinski, *Environmental Profile, Accident Analysis and the Tritium Safety Case for a Multi-Kilogram Breeder Plant*, Kronos series 2.107, doi:10.5281/zenodo.22645754. https://www.kronosfusionenergy.com/publications/inherent-safety-and-environmental-case.html

11 P I Ford, *The Sub-100 MW Byproduct-Material Thesis: Why a Compact Spherical-Tokamak Breeder Licenses Under NRC 10 CFR Part 30 Rather Than Part 50*, Kronos series 2.108, doi:10.5281/zenodo.22645756. https://www.kronosfusionenergy.com/publications/licensing-byproduct-material-part-30.html

12 H-S Bosch and G M Hale, *Improved formulas for fusion cross-sections and thermal reactivities*, Nucl. Fusion **32** (1992) 611.

13 W M Nevins, *A review of confinement requirements for advanced fuels*, J. Fusion Energy **17** (1998) 25.

14 T H Rider, *Fundamental limitations on plasma fusion systems not in thermodynamic equilibrium*, Phys. Plasmas **4** (1997) 1039.

15 L J Wittenberg, J F Santarius and G L Kulcinski, *Lunar source of ^{3}He for commercial fusion power*, Fusion Technol. **10** (1986) 167.

16 R F Post, *The magnetic mirror approach to fusion*, Nucl. Fusion **27** (1987) 1579.

17 T K Fowler and B G Logan, *The tandem mirror reactor*, Comments Plasma Phys. Control. Fusion **2** (1977) 167.

18 V P Pastukhov, *Collisional losses of electrons from an adiabatic trap in a plasma with a positive potential*, Nucl. Fusion **14** (1974) 3.

19 R H Cohen, M E Rensink, T A Cutler and A A Mirin, *Collisional loss of electrostatically confined species in a magnetic mirror*, Nucl. Fusion **18** (1978) 1229.

20 D E Baldwin, *End-loss processes from mirror machines*, Rev. Mod. Phys. **49** (1977) 317.

21 G I Dimov, V V Zakaidakov and M E Kishinevsky, *Thermonuclear confinement with twin mirror systems*, Sov. J. Plasma Phys. **2**

COLOPHON

How this document was made

The Kronos Fleet — Combined Editorial, 2026 is set in **Fraunces** (display), **Gelasio** (text), and **IBM Plex Mono** (data & equations), carried forward from the Kronos editorial design system.

The figures are rendered at 300 dpi from the deposited generator scripts; the document is composed as a single self-contained file with embedded fonts and imagery, paginated to US Letter, and rendered to PDF through a headless Chromium engine in matched light and dark editions.

Every headline quantity carries an evidence class; withdrawn and restated values are marked as such. Nothing herein is frozen beyond the founder-approved Tier-A set.

Explore it live — turn the interactive 3-D model, run the deposited solvers in the physics validator, and watch the companion film series.

LEGAL NOTICE

Notice, status, and distribution

Conceptual design & simulation study. This document reports a conceptual design and simulation study. It is not a construction commitment, a safety-analysis report, a regulatory filing, or an offer of securities. Forward-looking statements — schedules, costs, market sizes, and performance — are estimates subject to the limitations set out in the Simulations part and may change.

Numbers and their classes. Quantities are reported with evidence classes and case labels; modelled, assumed, and requirement-class values are identified as such and are not to be quoted without their labels.

Public edition. This edition carries the physics and design only; all financial, funding, and defense-commercial content has been removed for public distribution. The scientific text corresponds to the arXiv and journal submissions.

THE 2026 KRONOS SERIES

One programme, many papers

This editorial is one paper in the Kronos 2026 series — a real fusion company's complete, reproducible physics record for a spherical-tokamak breeder and its low-neutron D–^{3}He tandem-mirror burners. Every headline number is a frozen anchor in the Physics De-Risking Register.

Explore the whole programme: the De-Risking Register, the interactive 3-D model, and the physics validator.

KRONOS FUSION ENERGY

The Neutron-Lean Siting Case for a D–^{3}He Tandem-Mirror Burner: Parasitic D–D/D–T Neutron Budgets, Shielded Housing Dose, and Tritium-Suppressed Operation for Defense and Urban Deployment

A real fusion company building real machines. Explore the science, live.

Zenodo · doi:10.5281/zenodo.22645917

Read on kronosfusionenergy.com

The Physics De-Risking Register